

What's next in Nuclear Physics with RIB's

Björn Jonson

Fundamental Fysik, Chalmers Tekniska Högskola, SE-412 96 Göteborg, Sweden

Received: date / Revised version: date

Abstract. The physics with energetic radioactive beams has had a tremendous development over the 30 years that have passed since Isao Tanihata's famous experiments at Berkeley. The lectures presented in our school bear beautiful witnesses about this. The experiments and the subsequent understanding that halo structure occur for some very exotic nuclei have attracted so much interest and given so many novel ideas that one may speak about a paradigm shift. I shall here give some, personal, ideas about "What's next". This is an interesting task and I shall not say that it is difficult but rather challenging. I shall, however, start by giving a few milestones, preceding the 1985 break-through, that were of key importance for creating our sub-field of modern nuclear physics.

PACS. PACS-key describing text of that key – PACS-key describing text of that key

1 Introduction

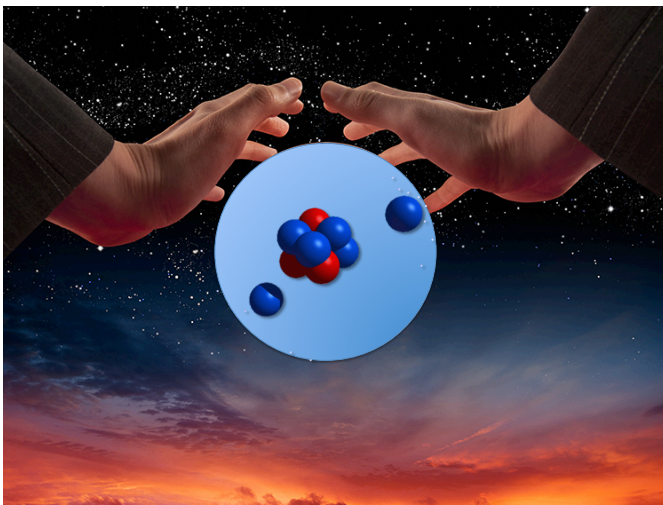


Fig. 1. To speculate over what comes next in the physics with radioactive beams is a daring feat. The rôle of the exotic nucleus ^{11}Li in our school makes it the obvious centre in the prophecy of the future, since it has been quite in focus over the past 30 years.

Our school has now come to its end. It is my duty to give you some hints of what comes next in this very active field on modern nuclear physics. I shall do this to the best of my knowledge. We have witnessed a spectacular development of the science utilising radioactive nuclear

Send offprint requests to:

beams, or as they often are referred to rare isotope beams (RIBs), over the 30 years that have passed since the first experiment was performed. We have heard Isao Tanihata telling about how the search for *anomalons* gave strange results for the Li and He interaction cross sections. Results that triggered the idea of a halo structure in exotic nuclei.

When my good friend and colleague Angela Bonaccorso first told me about her plans to make an effort to introduce the most modern concepts in the teaching of nuclear physics, I immediately became very interested. There has for many years been a lack of textbooks that keep up with the latest developments in our field. Some very recent discoveries can obviously not directly enter in the curriculum. But some things are now so central that teaching without mentioning them would be wrong.

The idea to select an anniversary as a start to create a new textbook is excellent. And no other nucleus than ^{11}Li could be a better ambassador for this work since it has been around all the time from the beginning 30 years ago and since it is still going strong. It was with 790 MeV/u beams of $^{6-9,11}\text{Li}$ that interaction cross sections were measured and matter radii deduced. The surprise was the huge increase in the matter radius for the last particle-bound isotope, ^{11}Li [1]. Further, it was the rich source of open beta-delayed particle branches in ^{11}Li that indirectly led to the understanding of the presence of nuclear halo structure [2]. It is also in ^{11}Li that we today can find evidence for an isoscalar resonance, as described in the beautiful paper by Kanungo *et al.* [3]. If you could tell the future by looking into a crystal ball, it would be obvious that the crystal ball of our field is the Borromean two-neutron halo nucleus ^{11}Li (Fig. 1).

We have during this week heard eleven beautiful lectures covering the state of the art of our field. Together

with the needed basic concepts the lecturers glimpsed into some new and burning issues that they are occupied with in their daily research work.

One basic question is where the borders of the nuclear chart are situated. For that, isotopes of the elements all the way out to the end of existence on both sides of beta stability have to be identified. We speak about the proton and neutron *driplines*, that is a limit where no more proton/neutron can be bound to the nucleus - they simply drip off. To keep track of all experimental data existing for the variety of different isotopes there are many compilations. A novel approach was taken by M. Thoennessen, who in the year 2007 started the "*Discovery of Nuclides Project*" [4]. With painstaking effort members of the project has listed the authors of papers reporting the first observation of each known isotope. The superstar here is H. Geissel, working at GSI, who has co-authored papers dealing with the discovery of 272 isotopes. It is also interesting to note that F.W. Aston (Nobel Prize in chemistry 1922 for "*for his discovery, by means of his mass spectrograph, of isotopes, in a large number of non-radioactive elements, and for his enunciation of the whole-number rule*") still belongs to the top quartet.

Before continuing with the hot issues of our time I shall in the next section stress the importance of some experiments that have strongly influenced our field and been of key importance for its future development.

2 The Halo prehistory

At the end of the forties relatively few radioactive isotopes had been discovered. Important ingredients in the studies of their structure were investigations of nuclear properties as a function of mass (isobars), number of neutrons (isotopes) or protons (isotones). For this a need for nuclei with additional combinations of protons and neutrons was obvious. With the advent of particle accelerators this wish was to some extent fulfilled but had its limitations in how fast one could produce, purify and undertake a measurement on a certain radioactive isotope. The limit was the nuclear half-life!

The first milestone I would like to mention is a pilot experiment performed as far back as in 1951 by O. Kofoed Hansen and K-O Nielsen at the Institute for Theoretical Physics at the University of Copenhagen (today The Niels Bohr Institute) [5]¹. Kofoed Hansen was interested in testing Paulis neutrino hypothesis in beta-decay experiments. To avoid chemical effects he studied the decay of noble-gas elements. To extend his studies to short-lived nuclides a new production technique, where an isotope separator was linked directly to the Copenhagen cyclotron, was developed, see Fig. 2. The great success of the Copenhagen experiments was that the production method was shown to work and a number of formerly unknown isotopes of the el-

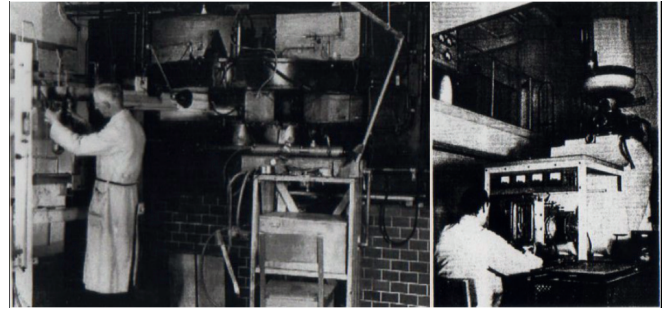


Fig. 2. The cyclotron (left) and the isotope separator (right) at the Institute for Theoretical Physics in Copenhagen. A uranium target, irradiated with neutrons produced in an internal beryllium target in the cyclotron, was directly connected to the ion-source of the isotope separator. In this way short-lived isotopes not earlier possible to produce fast enough were obtained. With this the so-called ISOL method was born.

ements krypton and xenon were identified². The main aim of the experiment was to extend the number of beta emitters to learn more about the neutrinos. Today we know that most important for our future was the demonstration of the feasibility of the ISOL method.

The Pontecorvo–Maki–Nakagawa–Sakata matrix

$$U = \begin{bmatrix} U_{e1} & U_{e2} & U_{e3} \\ U_{\mu1} & U_{\mu2} & U_{\mu3} \\ U_{\tau1} & U_{\tau2} & U_{\tau3} \end{bmatrix} = \begin{bmatrix} 1 & 0 & 0 \\ 0 & \cos\theta_{23} & \sin\theta_{23} \\ 0 & -\sin\theta_{23} & \cos\theta_{23} \end{bmatrix} \begin{bmatrix} \cos\theta_{13} & 0 & \sin\theta_{13}e^{-i\delta} \\ 0 & 1 & 0 \\ -\sin\theta_{13}e^{-i\delta} & 0 & \cos\theta_{13} \end{bmatrix} \begin{bmatrix} \cos\theta_{12} & \sin\theta_{12} & 0 \\ -\sin\theta_{12} & \cos\theta_{12} & 0 \\ 0 & 0 & 1 \end{bmatrix} \begin{bmatrix} e^{i\theta_{12}/2} & 0 & 0 \\ 0 & e^{i\theta_{12}/2} & 0 \\ 0 & 0 & 1 \end{bmatrix}$$

Atmospheric Accelerator Reactor Sun Reactor $\beta\beta$ decay

Fig. 3. The neutrino mixing matrix. The physical neutrinos, the flavour eigenstates, ν_e, ν_μ and ν_τ , are not identical to the mass eigenstates ν_1, ν_2 and ν_3 and are connected with an unitary matrix U . A neutrino with flavour α can then be written

$$|\nu_\alpha\rangle = \sum_{i=1}^3 U_{\alpha i}^* |\nu_i\rangle.$$

The mixing matrix may be decomposed as shown, which is useful since it turns out that experimental data can be analysed, to a good approximation, in terms of oscillations between just two neutrino flavours. With atmospheric neutrinos ν_μ the Kamioakande experiment determined the mixing angle θ_{23} while the solar neutrinos ν_e were used to determine θ_{12} at the SNO experiment. The last line gives which type of experiment that are sensitive to each sub-matrix. See also Ref. [12].

¹ The acknowledgement in Ref. [5] is interesting. It begins with... "We wish to thank Professor N. Bohr for his interest taken in our work ..."

² These investigations were part of the thesis work of Kofoed Hansen [6], a brilliant thesis summarising his studies in nine pages only!

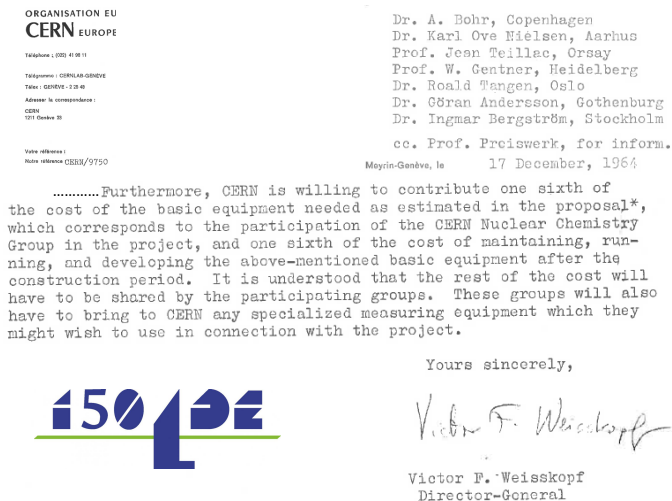


Fig. 4. The letter from W.F. Weisskopf to the ISOLDE Community in 1964. Note that the first addressee is the 1975 Nobel laureate A. Bohr.

When we are here together at Largo Bruno Pontecorvo it is interesting to see how neutrino physics has developed over the years. Pontecorvo was the pioneer by his neutrino-oscillation prediction [7,8], which today is on such a solid experimental footing. The results from Kamiokande [9] and SNO [10,11] were the key experiments that showed the presence of neutrino oscillations and today all the mixing angles have been determined, see Fig. 3.³

Inspired of the success of the Copenhagen experiment, the European nuclear-physics community proposed to build a general-purpose experiment for ISOL production of short-lived isotopes connected to the 600 MeV proton synchrocyclotron (SC) at CERN. An international collaboration was formed and a proposal was sent to CERN in 1964. The Director-General W. Weisskopf, approved this proposal (Fig. 4) and experiments, under the name ISOLDE, started [13].

An important step towards creating a community of physicists with interest in the opportunities offered by on-line production of radioactive isotopes was a conference held in Lysekil, Sweden, in 1966 [14]. The prospects for the future possibilities were discussed and many of the ideas for new experiments discussed during the Conference became realities during the coming decades. As a curiosity, in the concluding discussion [15], J.P. Bondorf stated "the rich field of information that would be opened by a future use of unstable targets and *projectiles* in nuclear reaction studies." The idea of creating radioactive beams has thus been with us from the very beginning, almost 50 years ago.

³ During the writing of this contribution we were happy to announce that the Nobel Prize for Physics 2015 was awarded to Takaaki Kajita from the Super-Kamiokande Collaboration and Arthur B. McDonald from the Sudbury Neutrino Observatory Collaboration for "for the discovery of neutrino oscillations, which shows that neutrinos have mass." [12].

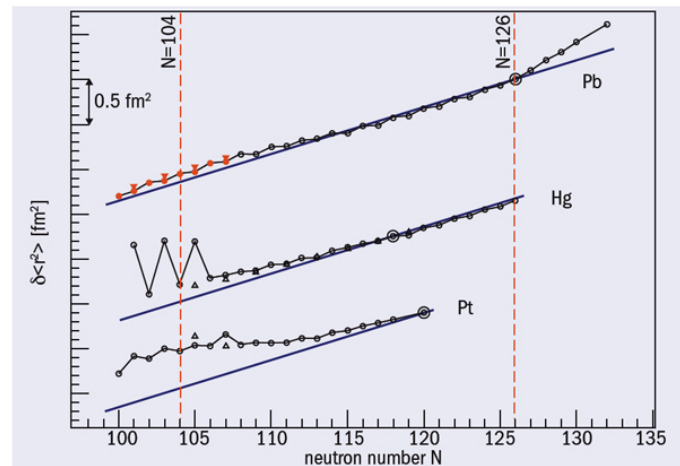


Fig. 5. Relative change in mean-square nuclear charge radii, $\delta \langle r^2 \rangle$, for the even- Z $_{80}\text{Hg}$, $_{82}\text{Pb}$ and $_{84}\text{Po}$ isotopes. While the relative change in charge radii of one isotope compared to its neighbour for the heaviest isotopes are very similar for these three elements, large differences are observed further away from the $N=126$ neutron shell closure. The large staggering observed in the Hg data is interpreted as shape coexistence caused by the occupation of specific single-particle states. The deviation observed for the Po isotopes is linked to an onset of collective behaviour possibly caused by the same mechanism. Adapted from Ref. [18].

The underground hall at ISOLDE was ready in 1967 and the first experiments were performed in October the same year. The experiments were immediately successful and the Collaboration could identify several new isotopes of the elements argon, krypton, silver, cadmium, tin, iodine, xenon, platinum, gold, mercury, polonium, radon and francium [16].

The second important development with a major impact on the physics on exotic nuclei was an experiment at ISOLDE, proposed in 1968, using atomic techniques. The experimental method, referred to as RADOP (Radioactive Detection of Optical Pumping), was based on optical pumping with the use of a mercury lamp. A most surprising result was obtained when the isotope shifts for the light mercury isotopes were measured. These shifts, that reflect the change in the nuclear charge distribution, showed that the root-mean-square radii differ significantly from the traditional expression $\langle r^2 \rangle^{1/2} = R_0 A^{1/3}$, where R_0 is approximately constant and A is the mass number. Instead it was found [17] that the radius of ^{185}Hg was significantly larger than that of ^{187}Hg . The results for even lighter mercury isotopes showed later a drastic odd/even staggering. These results are now well understood as shape coexistence caused by the occupation of specific single-particle states (see Fig. 5). But at the time this unexpected result was, however, very important for whole ISOLDE collaboration, since it attracted a lot of interest from CERN and also from the nuclear physics community.

The ISOL technique had a lot of successes during the seventies and eighties. There is, however, a series of experiments performed at Berkeley in 1979 that opened up another technique for production of exotic isotopes. Symons and Westfall [19,20] showed the feasibility of producing exotic nuclei with a beam of heavy ions. The success was great but Symons was very careful when he presented the results during the Helsingør Conference in 1981, when he concluded his talk by saying: "...we questioned the applicability of high energy heavy ion accelerators to this field. Our experience at the Bevalac leads us to believe that this question does indeed have a positive answer. If the physics interest justifies it, then high energy heavy ion beams can certainly be expected to play a role in the study of nuclei at the limits of stability..." [21]. Today we know that the In-Flight technique is dominating in the production of new exotic isotopes....

The heaviest particle-stable lithium isotope, ^{11}Li , was first observed in an experiment at Berkeley by Poskanzer *et al.* [22]. It was also found that ^{10}Li was unbound [23]. In an experiment at the CERN PS, Robert Klapisch and his group from Orsay set up an experiment to produce and study Li isotopes and, in particular, to measure their masses [24].

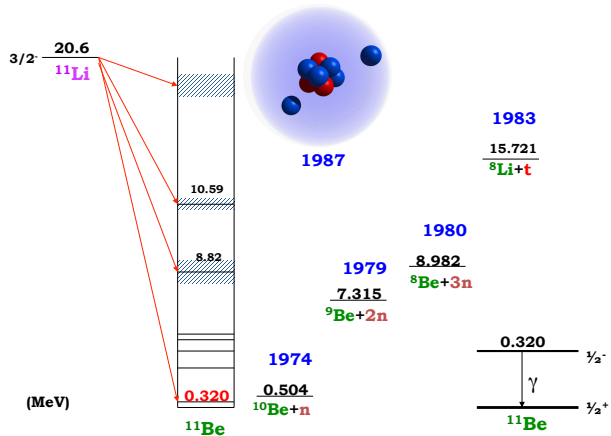


Fig. 6. Schematic decay scheme for the two-neutron halo nucleus ^{11}Li showing its major beta-delayed particle decay modes (with indications of the year of their discovery) The upper inset is a cartoon of its halo structure and the lower shows the bound levels in its beta-decay daughter, the one-neutron halo nucleus ^{11}Be .

At ISOLDE the development of a new target type with a target matrix consisting of uranium carbide, UC, gave interesting opportunities to study isotopes from many different elements produced in spallation, fission and fragmentation reactions. In particular high fragmentation yields giving Li isotopes were found. Here again ^{11}Li came into focus. With its very high Q-value for beta decay and the low separation energies for a variety of possible beta-delayed

decay modes it gave interesting prospects for new experiments as illustrated in Fig. 6. The presence of beta-delayed neutrons had already been observed [25] and at ISOLDE the focus became the more exotic decay modes, starting with beta-delayed two-neutron emission [26] and beta-delayed three-neutron emission [27].

Here it is maybe educative to give some details about these experiments and their analysis. The ^{11}Li radioactivity was separated on-line in the ISOLDE facility and directed as an ion beam to the centre of a paraffin-filled 4π -neutron counter. The neutron counter was equipped with a total of 12 ^3He tubes, which gave a detector efficiency of $(20 \pm 1)\%$. The residence time in the detector, as determined from beta-neutron coincidences on ^9Li , was exponentially distributed with a mean lifetime of $89 \mu\text{s}$. The neutron counters were connected in parallel and fed into a microprocessor unit that allowed the arrival times of individual neutrons to be read by a "flying clock" with a precision of $1 \mu\text{s}$. A time correlation analysis could then be performed in playback mode.

Assume a constant β -disintegration rate D decay through channels involving the emission of i neutrons with the probabilities p_{in} per β -decay. In most cases, however, only a single neutron will be detected, and it is therefore convenient to define the rates R_s of actual correlated events of s counts in the data string. If each multiplicity is characterised by an energy-independent average efficiency ϵ_i , we may then write

$$R_s = D \sum_{i=s}^{\infty} p_{in} \binom{s}{i} \epsilon_i^s (1 - \epsilon_i)^{i-s} \quad (1)$$

where $\binom{s}{i}$ is the binomial coefficient. The quantities R_s are then directly determined from a correlation analysis of the data and the ratios of the p_{in} values may subsequently be found by solving Eq. (1).

The strategy for detecting correlations is now to examine a time interval θ following an initial detected neutron. If $q-1$ neutrons have been recorded during the time interval, the event is registered as a q -fold event. For an individual count belonging to the event, the detection probability per unit time is $\lambda e^{-\lambda t}$, where $1/\lambda$ ($=89 \mu\text{s}$) corresponds to the mean residence time in the counter. With this strategy the (true) counting rate of q -fold events is

$$M_q^{(t)} = \sum_{s=q}^{\infty} R_s r_{s,q}, \quad (2)$$

where $r_{s,q}$ is the probability of exactly $q-1$ counts out of $s-1$ possible are falling inside the time window

$$r_{s,q} = \binom{s-1}{q-1} (1 - e^{-\lambda\theta})^{q-1} e^{-\lambda\theta(s-q)} \quad (3)$$

The contribution from random events, $M^{(r)}$, can be calculated as combinations of events of lower multiplicity. The expression for random doubles (1^2) is:

$$M_2^{(r)} = R_1^2 \theta \exp(-R_1 \theta) \quad (4)$$

and for random triples (2-1) and (1³)

$$M_3^{(r)} = R_1 R_2 \theta \exp(-R_1 \theta) \quad (5)$$

$$\times [2 - \exp(-\lambda \theta) - (1 - \exp(-\lambda \theta)) / \lambda \theta] \quad (6)$$

$$+ \frac{1}{2} R_1^3 \theta^2 \exp(-R_1 \theta) \quad (7)$$

It is then possible, from the measured $M_q = M_q^{(t)} + M_q^{(r)}$ to solve the equations for the R_s . The result is shown in Fig. 7.

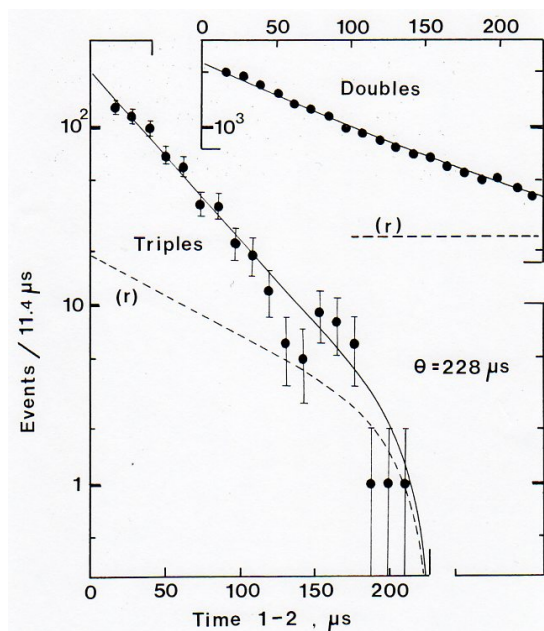


Fig. 7. Distribution of the time interval between the first and the second neutrons for events registered as doubles and triples with a correlation time $\theta = 228 \mu\text{s}$ after beta-decay of ^{11}Li . The theoretical curves showing the total number of events and the contribution from random events (dashed, r). Note that for triples events, when the first neutron is detected, the probability to detect one more neutron is twice as large. The curve in the inset clearly show the then expected $e^{-2\lambda t}$ dependence.

The ^{11}Li energy window for beta-delayed decays included also the possibility to observe beta-delayed triton emission. A successful identification of this rare decay mode was done in 1983 at ISOLDE [28].

The photo from the ISOLDE control desk (Fig. 8) shows some of the people involved in different experiments on ^{11}Li at the end of the seventies and the beginning of the eighties.⁴

⁴ This was at a time when a referee report, even from a competitor, could be as short as one single sentence. There were no politically stopping or delaying of papers to get priority. One could hope that "What comes next" is that we return to such a friendly competition and give support each other again. Or is this too much of a dream?



Fig. 8. The ISOLDE control desk in the beginning of the eighties. Upper row: R. Fergeau, F. Touchard and A. Poskanzer (author of the paper reporting the discovery of ^{11}Li). Lower row: B.J., P.G. Hansen, S. Mattsson (fellow) and R. Klapish (scientific director at CERN and former leader of the group studying ^{11}Li at the CERN PS.)

Gregers Hansen and I were in 1986 invited to write a review article, "Beta-delayed particle emission from light neutron-rich nuclei" [29], a review that was felt to be very timely mainly due to the successes with new observed decay modes from ^{11}Li . We had already seen the paper by Isao Tanihata and his team [1] and the stunning result attracted our curiosity. We suggested that the result could be explained as a neutron halo formed as a consequence of the low binding energy of the last neutron pair in ^{11}Li . We submitted a paper entitled "The neutron halo of extremely neutron-rich nuclei" to the, at that time relatively new journal, *Europhys. Lett.* [2]. This became also for us the start of an intense experimental activity.

I shall now return to my task and give some examples on future trends in our field.

3 Some upcoming experiments

Fig. 9 illustrates some of the subjects that have been in focus for experimental and theoretical investigations over the past 30 years. Most of the issues indicated around the chart of nuclides are still in the forefront of the interest and the RIB physics has played a major rôle in the experiments. I shall give several examples of very recent and upcoming experiments in the following.

Before that I want to point to one aspect of the contemporary physics that have evolved in an accelerating fashion over the past one or maybe two decades. Frontline research in subatomic physics is today strongly dependant of modern information technology. Modern theory with advanced models for the structure and dynamics of the atomic nucleus is one of the most demanding challenges in computing technology in current research. Also

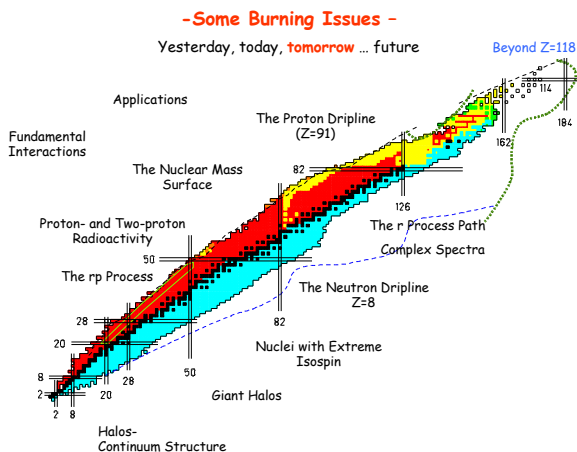


Fig. 9. Nuclear chart with some of the "hot" RIB physics issues that have been in focus over the past 30 years. In particular the region of the lightest nuclei has been subject for many different experimental investigations. The dripline has been reached for neutron-rich nuclei up to $Z = 8$, while the proton dripline has been delineated up to the element bismuth ($Z = 83$) by, for example, studies of proton radioactivity [30].

experiments performed at the internationally leading nuclear physics research facilities generate data of amount and complexity that asks for effective and creative data evaluation. Collaboration with front-line expertise in information technology concerning hardware, software and algorithms is therefore of great interest. As illustrated in Fig. 10 there is a strong interplay between experiment-theory and what we may refer to as eScience. eScience is today widely accepted and has developed into a field of itself. There are, however, a clear need for both experiments

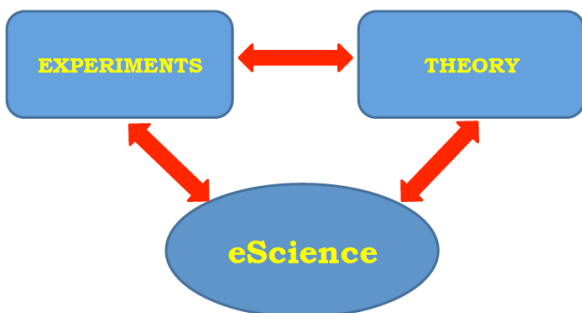


Fig. 10. The more and more central rôle played by high-level computations in subatomic physics creates a need and an opportunity to open collaborations with information technology experts.

and theory to participate in this endeavour. Most of the research activities in e-Science have focused on the development of new computational tools and infrastructures to support scientific discovery. Due to the complexity of the software and the infrastructural requirements, e-Science projects usually involve large teams managed and developed by research laboratories, large universities or governments. The link to our modern society is thus not far away.

3.1 New and upgraded Facilities

There has never before, in the history on nuclear science, been such a rapid development of new and upgraded research facilities as we witness today. We can distinguish two main methods of production of energetic radioactive beams:

- (i) the ISOL method with post-acceleration of the produced radioactive beams and
- (ii) the In-Flight method

illustrated in Fig. 11. In Europe the REX-ISOLDE Facility [31] is an example where radioactive beams up to 3 MeV/u has been utilised with great success since its start of operation in 2001. A new project, HIE ISOLDE, was approved in 2009. This project was the obvious next step in order to match the requirement of increasing the energy and intensity of the delivered radioactive ion beams. More energetic post accelerated beams are obtained by means of a new superconducting (SC) linac based on Quarter Wave Resonators (QWRs). In the short term the new accelerator modules will boost the energy up to 5.5, 8 and 10 MeV/u, while in

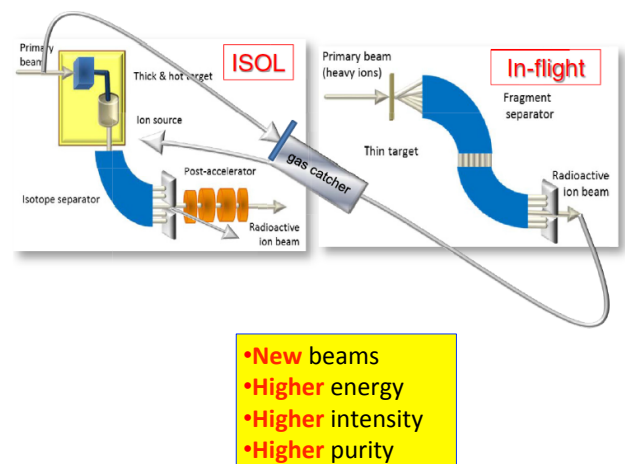


Fig. 11. The two main methods for production of radioactive nuclei. The ISOL and the In-Flight methods (from Ref. [32]). The construction efforts of the new and upgraded facilities have some common goals: One wants new beams, higher energy (or possibility to tune the beam energy optimally), higher primary beam intensity to increase the production of exotic nuclei and, finally, higher purity.

the longer term, part of present normal conducting linac will be replaced by new superconducting cavities in order to give beam energies that can be varied between 1.2 and 10 MeV/u. The first experiment, planned for autumn 2015, is a study of Coulomb excitation of ^{60}Zn . With beam energy of 260 MeV (4.3 MeV/u) from HIE-ISOLDE the experiment will use multi-step Coulomb excitation in the safe Coulex mode. The transition strength $B(E2\uparrow)$ in the ground-state band will be used to extract the deformation parameters of the low-lying excited states of ^{60}Zn . The experiment setup include the highly-efficient MINIBALL γ spectrometer coupled to a *DSSD* Si detector.⁵

Second, a study of the transfer reaction $^9\text{Li}(d,p)^{10}\text{Li}$ and then, in a next step when the energy is high enough, to extend the studies to excited resonance states in ^{11}Li . This will be done using a radioactive target in $^9\text{Li}(t,p)^{11}\text{Li}$ reactions.

It is also interesting to use the possibility to stop In-Flight produced isotopes in a linear gas catcher prior to a new acceleration, as illustrated in Fig. 11. A novel concept to stop the fast beams is to use a gas-filled reverse cyclotron magnet shown in Fig. 12, which is under construction at future FRIB at MSU [33]. With this technique one avoids many limitations of the linear gas cells.

⁵ During the writing of this contribution a message came from CERN that the first RIB had been accelerated in HIE ISOLDE. From the ISOLDE e-log at 17.24h on October 22, 2015: "First RIB ($^{74}\text{Zn}^{25+}$) at the of XT01 at ~ 4.0 MeV/u"

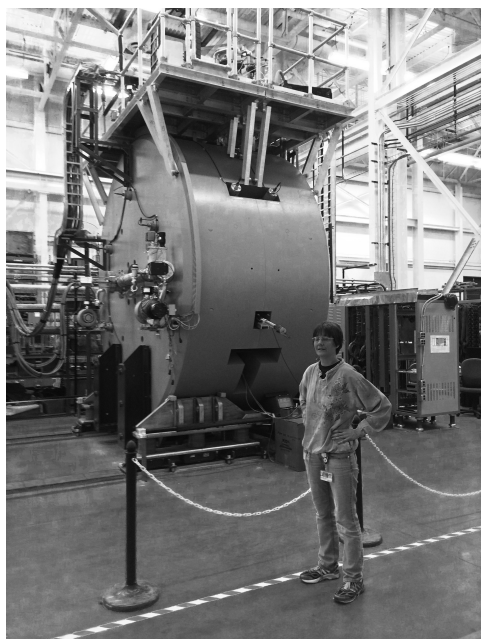


Fig. 12. Alexandra Gaade in front of the cyclotron gas-stopper magnet, which is a vertical superconducting split-solenoid configured into a focusing dipole with 120° radial symmetry. Photo: B. Jonson, April 23, 2015.

I shall now turn to the ongoing construction of SPES (Fig. 13)⁶, an acronym for Selective Production of Exotic Species at the Legnaro National Laboratory, where our school had an outing the final day. This project is devoted to basic research in nuclear physics and astrophysics as well as to interdisciplinary applications, ranging from the production of radionuclides of medical interest to the generation of neutrons for material studies, nuclear technologies and medicine. This is a project where I can foresee that many of the participating students in our school will have their future research activities, in particular those coming from Italy. It is a gift to have a National Laboratory of this class and we are all locking forward to see how it will develop.

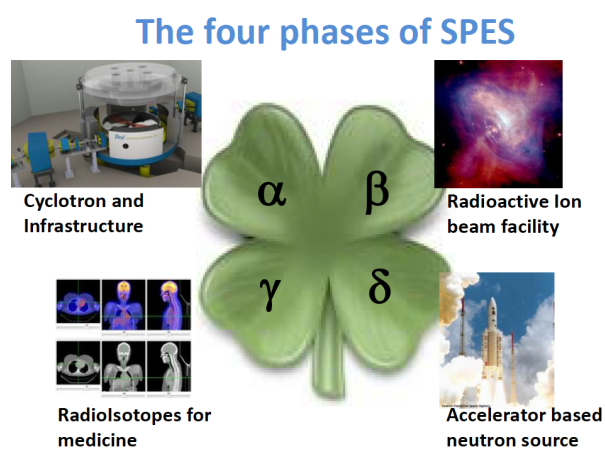


Fig. 13. (α) At the heart of SPES: the cyclotron and ISOL target (β) The acceleration of neutron-rich unstable nuclei (γ) Production of radionuclides for applications (δ) Multidisciplinary neutron sources

3.2 Detectors

Today our field is also in a period of very rapid development of equipment to be used in the next generation of experiments. As an example Fig. 14 shows the R3B setup planned to be erected in an external beam line after the new Super FRS Separator at the future FAIR Facility at the present GSI.

Waiting for the beams to appear at the new Facilities I can give two examples of experiments where detectors to be used at FAIR are utilised in experiments at ISOLDE and at RIKEN. In one experiment 20 neutron detectors from the MODular Neutron time of flight SpectromETER (MONSTER) for DESPEC experiment at FAIR were used at ISOLDE, CERN for a detailed study of the beta-delayed neutron branches from ^{11}Li . Another example is when four out of the 30 planned detector planes of

⁶ SPES is the hope of the laboratory as its Latin name implies.

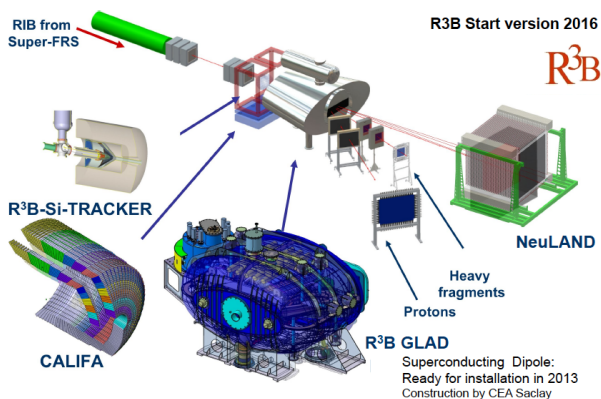


Fig. 14. The R³B experimental setup is versatile reaction setup with unprecedented efficiency, acceptance, and resolution for kinematically complete measurements of reactions with high-energy radioactive beams. The experimental configuration (initial setup, see Figure), is based on a concept similar to the existing R3B/LAND reaction setup at GSI introducing substantial improvement with respect to resolution and an extended detection scheme, which comprises the additional detection of light (target-like) recoil particles and a high-resolution fragment spectrometer.

the NeuLAND neutron detector (see Fig. 15) were brought to RIKEN for tests and experiments while waiting for beams at FAIR. Several experiments are planned at RIKEN during the coming years. One interesting study is to try to confirm the claimed and surprising observation of neutron radioactivity from ²⁶O, as well as the possible existence of a ²⁸O, a system with possible doubly-magicity and a structure of four neutron outside an ²⁴O core. A challenge....

When the NeuLand detector is fully equipped with its thirty planes the efficiency for detection of four simultaneous neutrons is as much as 63 % at 1000 MeV. With such an efficiency and the complete R3B setup this will open huge possibilities to study exotic decays.

3.2.1 Optical Time Projection Chamber

An example of a rather novel technique that certainly will be utilised in several experiments in the near future is based on an optical time projection chamber (OTPC) technique. In a recent experiment at REX-ISOLDE the rare beta-delayed particle emission process of the Borromean nucleus ⁶He into the $\alpha + d$ continuum was studied [34]. Bunches of post-accelerated ⁶He ions were implanted into the optical time projection chamber (OTPC), where the decays with emission of charged particles were recorded. This allowed to investigate the low-energy end of the particle spectrum down to 150 keV in the $\alpha + d$ centre of mass, corresponding to a deuteron energy of 100 keV (see Fig 16). The active volume of the chamber is filled with a mixture of 98% He and 2% N₂ at atmospheric pressure. A constant and uniform electric field is applied



Fig. 15. Left: Neutron detectors, to be used at FAIR, during a recent experiment on ¹¹Li at ISOLDE. Photo: B. Jonson. Right: Neutron detector planes for the future NeuLAND at FAIR shipped to RIKEN for measurements of ^{26–28}O.

over the detector. Through a kapton window ions enters and stops inside the gas. Both the entering ions and the charged particles emitted in the decay ionise the gas and the primary ionisation electrons drift in the electric field with a constant velocity towards the charge multiplication stage composed of four GEM foils and a wire mesh anode. The OTPC technique allows to study very rare decays with emission of charged particles, such as two-proton radioactivity, or β -delayed multi-particle emission and will certainly be very active in the coming years

3.2.2 The nuclear mass surface

Measurements of nuclear masses have over the years gone hand in hand with the technical developments to produce

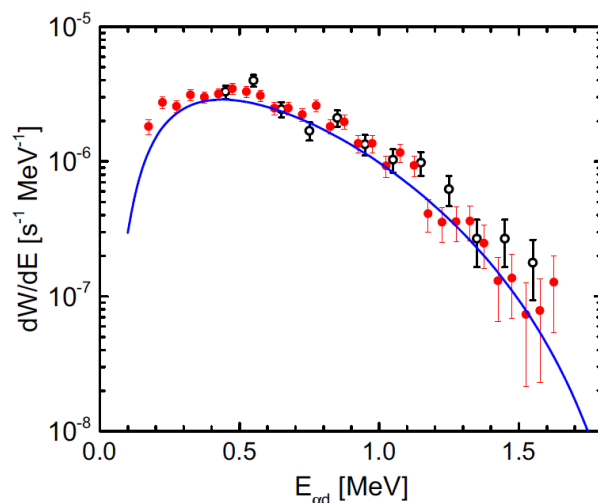


Fig. 16. Transition probability of the $\alpha + d$ branch in the β decay of ⁶He as a function of the $(\alpha + d)$ energy $E_{\alpha+d}$.

new radioactive beams. With a continuous and never decreasing ingenuity clever and advanced techniques have been developed [35]. Let me first give one example, which is relevant for our school: The two-neutron separation energy in ^{11}Li was, when we wrote our halo paper in 1987, known as 190(110) keV [24]. Today the value is 369.15(65) keV, obtained with the mass spectrometer TITAN at TRIUMF [36].

The precise mass data have many interesting applications. As an example one may take the isobaric mass equation, where nuclei with the same mass, A , and total isospin, T , are related as

$$M(\alpha, T, T_z) = a(\alpha, T) + b(\alpha, T)T_z + c(\alpha, T)T_z^2. \quad (8)$$

where the isobaric states are denoted (α, T, T_z) where α is the relevant quantum numbers (I^π, A) . The coefficients, a, b and c can be determined from experiments. Broken isospin invariance by non-electromagnetic interactions would result in higher order terms in the Eq. 8. Such terms would reflect the amount of isospin mixing and this was believed to be the case for the $A=20$ quintet, after recent new and very precise mass data for the isotope ^{20}Mg [37]. These data completed the $A=20$ multiplet and gave first evidence for a deviation from the quadratic IMME. But recent new gamma data following the super-allowed beta decay of ^{20}Mg gave a more precise value for the $T=2$ state in ^{20}Na [38] and resulted in a perfect fit to Eq. 8.

The mass spectroscopy groups, present at most major facilities, have given us access to the mass surface so that we today may "walk around on it" and look at all its fine details, like when Neil Armstrong was first to walk around on the moon in 1969.

3.2.3 Atomic techniques for measurements of spins and moments

Another type of measurements that follow production of new isotopes are those that use atomic physics methods for determining spins, moments and charge radii of the isotopes. Here I cannot resist telling a bit about the major

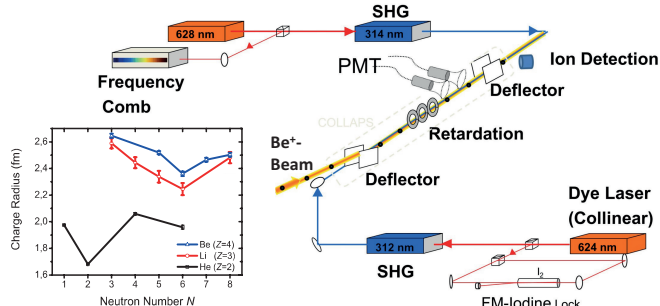


Fig. 17. Setup for collinear laser spectroscopy with parallel and antiparallel excitation and a frequency comb as reference for the determination of the charge radius for Be isotopes. The inset shows the state of the art of charge radii measurements [35] for light drip line nuclei.

experimental success that was given when the collinear laser technique was employed to determine the nuclear charge radii for Be isotopes. With a beam of Be^+ ions, a frequency comb and measuring the absolute transition frequencies for parallel and antiparallel geometry of the ion and laser beams a hitherto impossible precision was obtained (Fig. 17). The beauty of the technique is that the rest frame frequency, ν_0 , is obtained independent of the acceleration voltage by combining the measured absolute transition frequencies for parallel (ν_p) and antiparallel (ν_a) laser beams so that $\nu_p \nu_a = \nu_0^2 \gamma^2 (1 + \beta)(1 - \beta) = \nu_0^2$. The required accuracy in the isotope shift measurement of 1 MHz was obtained. The resulting charge radii are found to decrease for the isotopes ^7Be to ^{10}Be , but for $^{11,12}\text{Be}$ this trend is broken and an increase is found with $\delta < r_c^2 >^{10,11} = 0.49(5) \text{ fm}^2$ [39] and $\delta < r_c^2 >^{10,12} = 0.69(5) \text{ fm}^2$ [40], respectively. The increase for ^{11}Be may be ascribed as an effect of the difference in the centre-of-mass and centre-of-charge, while the increase for ^{12}Be is due to its deformation.

At FAIR the Super Fragment Separator (SFRS) is believed to provide a rich spectrum of isotopes that are not and will not be available at any other facility. From the view of optical spectroscopic research the facility will provide unique access to regions of particular nuclear interest that would otherwise remain inaccessible. The LASPEC Collaboration intends to perform experiments with for example collinear laser spectroscopy on ions, optical pumping and collinear laser spectroscopy on atoms, β -NMR. These are one type of new data expected when the FAIR facility gets beam.

3.2.4 Complex spectra and Pandemonium

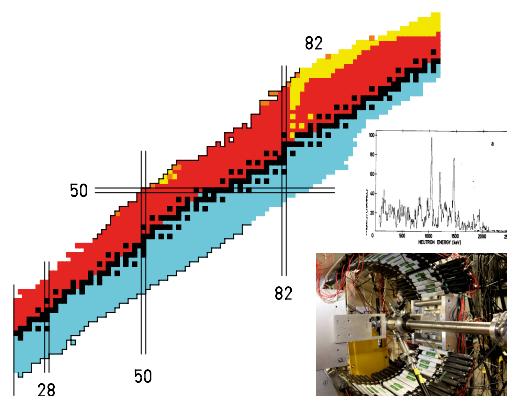


Fig. 18. Time-of-flight spectrometer for measurements of beta-delayed neutron spectra. The complexity of the decays of isotopes in the medium and heavy mass regions makes the analysis of the spectra complicated. In most cases the interpretations of the data are best done by adopting analysis employing a statistical model.

An experimental project for studies of beta-delayed neutron emission from medium-heavy elements is just starting at ISOLDE CERN. The Oak Ridge neutron detector VANDLE will be used along with the ISOLDE Decay Station (see Fig. 18). Neutron emission from $^{130,132}\text{Cd}$ is the first isotopes to be measured. These studies will later be extended to regions further away from magic proton and neutron numbers. One then becomes confronted with spectra that are very complex or even chaotic. One enters into a region known as the Pandemonium region. But what is Pandemonium?

Quite a few years ago a paper entitled "The Essential Decay of Pandemonium" [41] appeared. The idea was to investigate how reliable the analysis of very complex gamma spectra was. For that a fictional nucleus, using all physical ingredients, was created within a statistical model. These "data" were then analysed by the conventional methods as if they were real experimental data. The special feature was, however, that one knew what was behind the simulated spectra. This first paper about beta-delayed γ spectra demonstrated that the conventional analysis of the spectra left much of the intensity unobserved.

In a second similar paper [42] beta-delayed neutrons were simulated. The main ingredients in the simulation were the probability densities for the level spacings and the reduced transition probability. For the level density a Wigner [43] distribution gives the probability density of finding a given level spacing D between two neighbouring levels

$$P_W(s) = \frac{1}{2}\pi s \exp(-\frac{1}{4}\pi s^2), \quad (9)$$

where $s = D / \langle D \rangle$ is the spacing in units of the mean value.

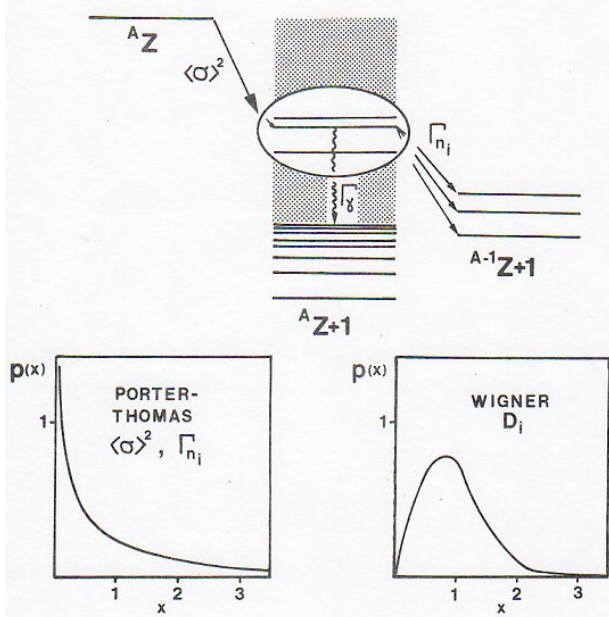


Fig. 19. The ingredients in the simulation of beta-delayed neutrons from the decay of Pandemonium [42].

The probability density to observe a transition probability γ^2 for a single reaction channel involving a final state f is according to Porter and Thomas [44]

$$P_{PT}(x) = (2\pi x)^{-1/2} \exp(-\frac{1}{2}x), \quad (10)$$

where $x = \gamma_f^2 / \langle \gamma_f^2 \rangle$ is the reduced transition probability in units of its mean value.

The beta-delayed neutron spectra from Pandemonium were then created by letting the level density follow a statistical model with a scattering according to the Wigner law. The individual intermediate states, fed in Gamow-Teller β decay, assumed to be constant on the average, were selected according to the Porter-Thomas law, as illustrated in Fig. 19. The subsequent decay of the intermediate states were assumed to be either γ or neutron decay. After folding with a Gaussian detector response function and including the effect of counting statistics the simulated spectra could be compared to experimental delayed neutron spectra. The outcome of this exercise was that there are many individual states contributing to the spectra and that the observed peak-like structure may contain contributions from many resonances.

The real number of involved resonances may then above a certain energy be hidden and the density of states involved in the beta decay is only reflecting intensity fluctuations governed by the Porter-Thomas law. If we look at the energy region where the total width, Γ , the level spacing D , and the experimental resolution $W_{1/2}$ are related as $\Gamma \ll D \ll W_{1/2}$ one may, in the case of particle intensity I and with a detector resolution $W_{1/2}$ according to Ref. [45] write

$$Var I = \sqrt{\frac{(2\ln 2)}{\pi}} \frac{I^2 D \alpha}{W_{1/2}} \quad (11)$$

where α , in the order 2 to 10, is the normalised variance. This means the one may derive the level spacing D when the overall energy spectrum $I(E)$ and the parameter α are theoretically understood.

Just to distinguish the the type of fluctuations we are concerned with here one may look at the autocorrelation function for Porter-Thomas noise for an infinite spectrum of unit intensity and a level spacing D , which reads

$$\begin{aligned} \psi_{PT}(\tau) &= \langle I(E)I(E+\tau) \rangle \\ &= 1 + \left(\frac{2\ln 2}{\pi}\right)^{1/2} \frac{\alpha D}{W_{1/2}} \exp[-2\ln 2(\tau/W_{1/2})^2]. \end{aligned} \quad (12)$$

Here the correlation width depends on the experimental resolution only and the level density is obtained from the correlation amplitude at $\tau=0$.

For fluctuations in the continuum, as investigated by Ericson [46], the autocorrelation function is

$$\psi_E(\tau) = \frac{1}{2T} \int_{-T}^T \sigma(E)\sigma(E+\tau)d\tau = \langle \sigma \rangle^2 \left(1 + \frac{\Gamma^2}{\Gamma^2 + \tau^2}\right)$$

for $T \rightarrow \infty$. When Γ is larger than $W_{1/2}$ the autocorrelation function will directly determine Γ and the level

spacing from the formula $\Gamma = \frac{D}{2\pi}N$, where N is the number of open channels.

A detailed outline how fluctuations in experimental beta-delayed particle spectra may be used to determine level density parameters is given in Ref. [47].

As an amusing detail one may calculate the number of maxima that appear in a noise spectrum given in Eq. 11. From the ratio of derivatives one obtains

$$\nu_{max} = \frac{1}{2\pi} \sqrt{[-\psi^{(4)}/\psi^{(2)}]_{\tau=0}} = \frac{(3ln2)^{1/2}}{\pi W_{1/2}} = \frac{0.456}{W_{1/2}} \quad (13)$$

where $\psi^{(i)}$ denotes the i th derivative with respect to τ and the ratio is evaluated at $\tau = 0$ [45]. With an energy resolution of 20 keV one would then observe about 20 maxima in a complex spectrum, independent of the number of underlying participating levels.

3.2.5 ${}^6\text{He}$ at the R3B setup at FAIR.

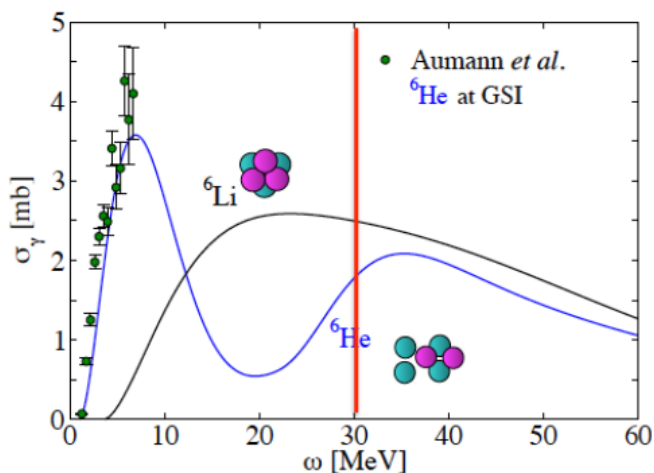


Fig. 20. Differential cross sections as a function energy for the ${}^6\text{He} \rightarrow \alpha + n + n$ reaction in a lead target. The curves are from Ref. [49] and the experimental data from Aumann *et al.*, [48]. The red line is the expected upper energy limit for experimental data at the future R3B setup. Courtesy Sonia Bracca.

In an experiment performed at GSI in 1999 the three-body breakup ${}^6\text{He} \rightarrow \alpha + n + n$ was studied with a lead target. The beam energy was 240 MeV/u and the experiment was utilising the ALADIN-LAND setup [48]. Fig. 20 shows the experimentally determined differential cross section, σ_γ , together with a calculation performed by Sonia Bracca and collaborators [49]. Six-body inelastic reactions was calculated microscopically including the full six-nucleon final state interaction. The calculated cross section for ${}^6\text{Li}$ shows one single broad giant resonance peak, while there are two well separated peaks for Borromean two-neutron

halo nucleus ${}^6\text{He}$, corresponding to the breakup of the neutron halo and the α core respectively (see Fig. 20). The experimental data extends, however, to 7 MeV only and the energy region where the interesting shape of the calculated ${}^6\text{He}$ breakup, with a decrease after the final available data point up to 20 MeV and then again an increase, is not yet available. Here the future will again be on our side since the new possibilities given by the R3B setup at FAIR with its GLAD magnet and higher energy (Fig. 14). The possible experimental limit will then be pushed up to about 30 MeV, well above the interesting energy region.

3.2.6 Heavy halos

Halo nuclei have been studied extensively over the almost thirty years since they were first observed experimentally. A recent review gives a summary of the present achievements [50]. The classical halos have mainly configurations with $2s$ or $1p$ orbits. In recent years the data have entered the $2p$ region, with ${}^{31}\text{Ne}$ being the first identified nucleus in this group. An interesting open question for the future is that since there are no quantum numbers preventing mixing between halos and other states one expect halo formation to be hindered as we move up in excitation energy to higher level densities. How such effects evolve as we move to heavier ground state halos is not yet clear but one may foresee that the coming generation of facilities may give us the experimental answer to this.

One way of classifying the halo states is to introduce dimensionless, universal scaling plots of radii versus binding energies for two- and three-body halo systems (see [50] and references therein). For a two-body halo, like ${}^{31}\text{Ne}$, one uses the mean square-distance, $\langle r^2 \rangle$, and the binding energy, B , and construct the dimensionless quantities $\langle r^2 \rangle / R^2$ and $\mu BR^2 / \hbar^2$, where μ is the reduced mass and R the scaling radius chosen as the equivalent square-well potential.

The usefulness of such scaling plots can be demonstrated for the ${}^{31}\text{Ne}$ case. Interaction cross-sections data for the chain of isotopes ${}^{20-32}\text{Ne}$ [51] revealed that all isotopes above $A=26$ exceed the normal systematic trend. In particular, the two cases ${}^{29}\text{Ne}$ and ${}^{31}\text{Ne}$ gave unusually large σ_I . The enhancements for these two isotopes suggest a dominant s -wave halo structure in ${}^{29}\text{Ne}$, which was interpreted as an s state with a $[200\ 1/2]$ Nilsson configuration. For the ${}^{31}\text{Ne}$ case, where an even stronger increase in σ_I was observed, $\ell=0$ or 1 orbitals with Nilsson numbers $[321\ 3/2]$ and $[200\ 1/2]$, depending on the neutron separation energy, S_n , was suggested. With the measured neutron separation energy of $S_n = 0.15^{+0.03}_{-0.1}$ MeV one may use the scaling plot to definitely assign an $\ell=1$ value for the ${}^{31}\text{Ne}$ halo, as shown in Fig. 21.

3.2.7 Delayed Particles

The very high energy available for beta decay for nuclei in the dripline regions, together with the generally low separation energies for nucleons or clusters in the daughter

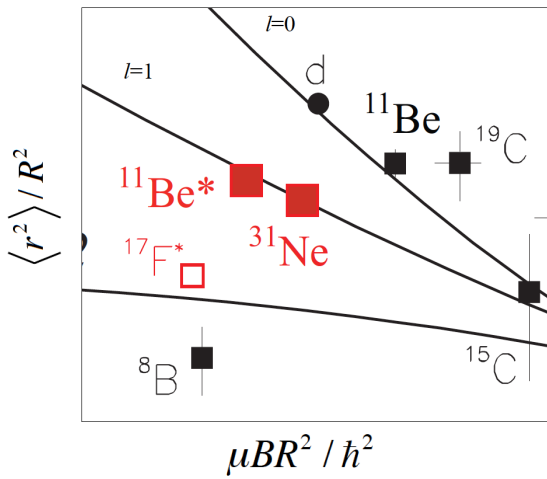


Fig. 21. Scaling plot for two-body halo systems. The filled circle is the deuteron and the filled squares were extracted from experimental interaction cross sections. The two red squares correspond to ${}^{11}\text{Be}$ and ${}^{11}\text{Be}^*$, which are the s -wave halo ground state and the p wave excited halo state, respectively. The ${}^{31}\text{Ne}$ data point shows that this is an $\ell=1$ halo state.

nuclei open the possibility for a variety of beta-delayed particle-emission processes. Fig. 22 illustrates this.

An interesting case is a beta-minus decay and followed by proton emission, which takes a nucleus in almost opposite directions on a nuclear chart, so that β^- delayed proton emission (where beta decay feeds excited states that subsequently emit a proton) is forbidden in all but a few nuclei, where it is heavily suppressed as the available energy only is

$$Q_{\beta-p} = 782 - S_n \text{ keV.} \quad (14)$$

Here S_n is the neutron separation energy.

The β^-p decay mode may be expected preferentially in one-neutron halo nuclei, partly due to the requirement

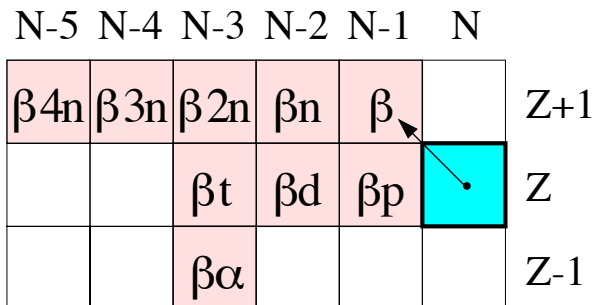


Fig. 22. Position of beta-delayed daughter nuclei on a nuclear chart.

of low neutron separation energy, partly due to the more pronounced single-particle behaviour of halo nuclei. One recently studied case at the ISOLDE isotope separator Facility is ${}^{11}\text{Be}$, with $S_n = 504$ keV, which gives $Q_{\beta-p} = 280$ keV. It is very hard to detect protons of such low energy and an alternative approach to find the branching for this rare decay mode was therefore employed. The beta decay from ${}^{11}\text{Be}$ feeds states in the daughter nucleus ${}^{11}\text{B}$ and, if the feeding goes to states in the upper 280 keV of the beta-decay window, a proton may be emitted. In the final state we have then a proton and a ${}^{10}\text{Be}$ nucleus. With a half-life of for ${}^{10}\text{Be}$ of $T_{1/2} = 1.6 \cdot 10^6$ a it is possible to try to detect the presence of ${}^{10}\text{Be}$ at the mass position $A=11$. To do this the group employed an AMS technique to detect the tiny amount of ${}^{10}\text{Be}$ [52]. The resulting branching ratio is $(8.3 \pm 0.9) \cdot 10^{-6}$, which is a surprisingly high branching since one from model estimates would expect it to be in the 10^{-8} region. The result may be interpreted as a quasi-free decay of the ${}^{11}\text{Be}$ halo neutron into a single-proton state. A continuation of this experiment is foreseen and a transfer experiment is planned to try to look for a possible proton resonance at the relevant energy in ${}^{11}\text{B}$.

3.2.8 Unbound Nuclei

Fig. 23 shows a part of the nuclear chart, where the squares given in green colour represent unbound nuclei, or resonances. In these cases one has been able to study their quantum properties. The progress of the understanding unbound nuclei has been spectacular over the past decades. The occurrence of a halo structure in ${}^{11}\text{Li}$, with a ${}^9\text{Li}$ core surrounded by two valence neutrons, and where the binary sub-systems ${}^{10}\text{Li}$ and nn are unbound could only be understood theoretically [53] if the unbound nucleus ${}^{10}\text{Li}$ has a s -wave ground state. This has been confirmed in

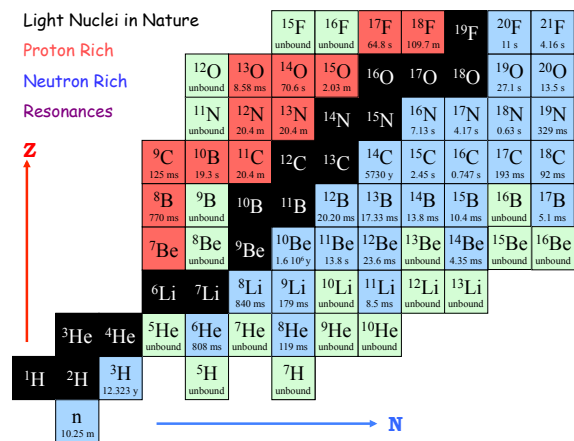


Fig. 23. Part of the chart of nuclides showing stable nuclei (black), proton rich (red) and neutron rich (blue) nuclei. The green squares represent unbound nuclei where experiments have been able to determine some of their quantum characteristics.

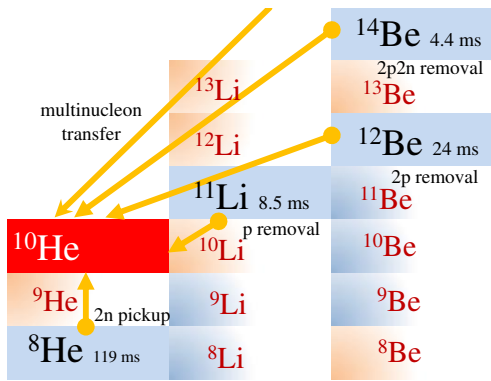


Fig. 24. The unbound ^{10}He nucleus may be produced in multi-nucleon transfer, α -, $2p$ - and $1p$ removal and $2n$ pick-up reactions. To draw conclusions of its structure it is important to consider different experiments and try to get a joint picture.

a number of experiments over the years, see for example Ref [54].

It is interesting to see how the experimental developments have made it possible to use nuclei close to the drip-lines, such as ^{11}Li and ^{14}Be , to create even more exotic systems in e.g. transfer or knockout reactions. With energetic beams up to relativistic energies one may perform studies in so called inverse kinematics where the exotic, short-lived nuclide is used as a beam, bombarding a stable target (see also the review by H. Simon [55]). For the production and study of the most neutron-rich isotope of the element He with mass ten, ^{10}He , it may be produced by for example proton knockout for ^{11}Li . Such an exotic system as ^{10}He need, however, much care to pin-point its structure and in order to gain a more complete understanding there is a need to take all different experimental data into account to try to get a general consensus of its structure, as illustrated in Fig. 24.

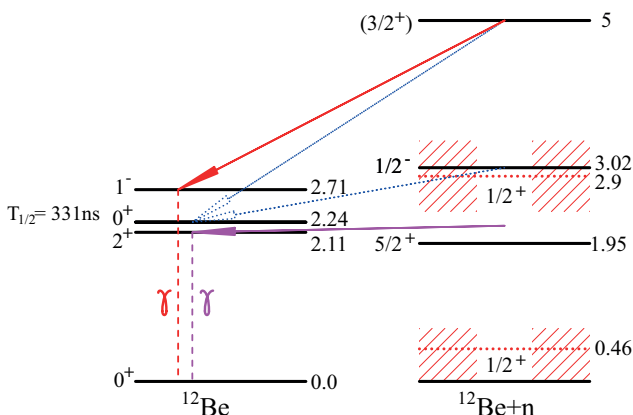


Fig. 25. Level scheme of states in ^{13}Be and ^{12}Be . The arrows show possible decays to excited states in ^{12}Be .

The unbound subsystems to the most neutron-rich light nuclei have maybe been especially in focus over the years.

For the ^8He , ^{11}Li and ^{14}Be the unbound subsystems are ^7He , ^{10}Li and ^{13}Be . Let me here just mention ^{13}Be . In the most recent experiments this nucleus has been produced in knockout reactions from ^{14}Be at GSI and RIKEN, while experiments at GANIL have utilised proton knockout from ^{14}B . All available data were collected in a recent paper [56] and the joint analysis gave a level scheme according to Fig. 25. The experimental consensus with the present available experimental data give the lowest-lying state, and then the ground state of ^{13}Be as a state with $I^\pi = 1/2^+$. Theoretically the situation is, however, not crystal clear. In a recent paper dealing with two-particle random-phase approximation it has been shown that the experimental characteristics of both ^{12}Be and ^{14}Be , such as two-neutron separation energies, RMS radii and other experimental determined quantities can be reproduced only if the orbit inversion persists across the threshold in ^{13}Be , which would give an s -orbit bound in the ^{12}Be core and with a p -wave resonance as the ground state of ^{13}Be (see Ref. [57] and references therein.).

More information about this open question about ^{13}Be may be given in a forthcoming experiment planned at the HIE ISOLDE Facility, where a beam of ^{11}Be will be used to study the two-neutron transfer reaction $^{11}\text{Be}(t,p)^{13}\text{Be}$. This additional information might shed more light over the very interesting ^{13}Be case!

The earlier mentioned experiment at RIKEN, will use invariant mass spectroscopy experiments to study the exotic oxygen isotopes beyond the last particle bound nucleus ^{24}O . In particular the possible doubly-magic nucleus ^{28}O and also the $N = 19$ nuclei ^{27}O and ^{28}F located beyond the neutron drip line would be studied in order to investigate shell evolution. These unbound nuclei are produced by one and two proton removal reactions of ^{29}F and ^{29}Ne on a thick liquid hydrogen target provided by MINOS at RIKEN. Decay products, outgoing charged particle and neutrons, are analysed by the SAMU-

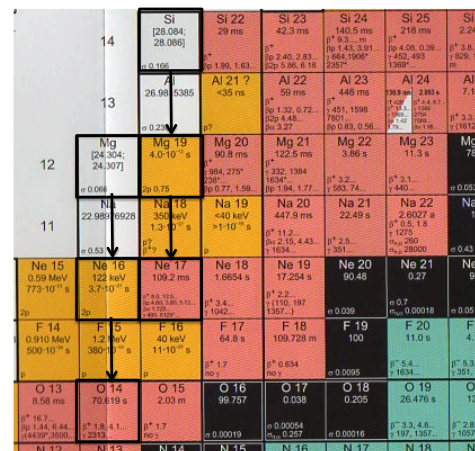


Fig. 26. Nuclear chart with in the region where two very exotic decays may be feasible. $^{21}\text{Si} \rightarrow ^{19}\text{Mg} + 2p \rightarrow ^{17}\text{Ne} + 2p$ and $^{18}\text{Mg} \rightarrow ^{16}\text{Ne} + 2p \rightarrow ^{14}\text{O} + 2p$.

RAI+NEBULA setup in combination with the four detector planes for the future NeuLAND detector at FAIR.

When the NeuLAND detector is fully equipped at the future R3B setup at FAIR the expected efficiency for detection of four simultaneous neutrons is about 63 %. With such an efficiency one obvious experiment is to look at ${}^7\text{He}$, which can be produced in proton knockout from ${}^8\text{He}$.

Even more exotic decays may be feasible in the future [58]. The first is a production of the unbound nucleus ${}^{18}\text{Mg}$, which would emit two protons to ${}^{16}\text{Ne}$, an in many respects interesting unbound nucleus [59–61] and then another $2p$ decay to ${}^{14}\text{O}$. The second is a similar decay ${}^{21}\text{Si} \rightarrow {}^{19}\text{Mg} + 2p \rightarrow {}^{17}\text{Ne} + 2p$ (see Fig. 26), where the intermediate nucleus is one of the known cases of $2p$ radioactivity [62, 63]. It will be very interesting to take deal of results from these two experiments, whenever they take place!

3.3 Electrons and antiprotons

The investigation of internal nuclear structure of short-lived radioactive nuclei by means of electron scattering is one type of studies just knocking at the door today. Electron scattering on exotic nuclei has not been possible due to the short half-lives, which exclude to make targets. At RIKEN an internal target system named SCRIT (Self-Confining RI Ion Target) has been developed and it is placed in an electron storage ring, which results in a nice and compact experimental system [64].

Another setup for electron scattering on exotic nuclei is planned at FAIR where the ElectronIon Scattering experiment (ELISe) has been studied as one future option at the Facility [65, 66] (see Fig. 27). ELISe will be a unique and unprecedented tool for precise measurements of nuclear charge distributions, transition charge and current matrix elements, and spectroscopic factors. This capabil-

ity will contribute to a variety of high-quality nuclear-structure data that will become available at FAIR.

We have also heard about the possibility to use antiprotons to probe exotic nuclei. The proximity of ISOLDE to the antiproton decelerator AD at CERN give for example interesting possibilities. With antiprotons one may study antiprotonic atoms and their subsequent annihilation process can yield important information on the mass radius and the proton-neutron composition on the nuclear surface.

At the future FAIR Facility there are also plans to use low-energy antiprotons in the FLAIR (Facility for Low-Energy Antiproton and Heavy Ion Research) project.

3.3.1 Nuclear astrophysics

The regions of the nuclear chart available for experimental studies has expanded very much over the past decades. One subfield of the research that has been of increasing importance in the programmes is experimental nuclear astrophysics with radioactive beams. A very complete overview of this research is given in the two reviews [67, 68].

To take one example one may consider the radiative capture reaction ${}^{12}\text{C}(\alpha, \gamma){}^{16}\text{O}$. This is extremely relevant for the fate of massive stars and determines if the remnant of a supernova explosion becomes a black hole or a neutron star. This reaction occurs at low-energies and an experimental study of it is very difficult or perhaps impossible. It is, however, well known that a study of beta-delayed α particles from ${}^{16}\text{Ne}$ gives a possibility to get the $E1$ component of the S factor for this reaction. In an upcoming experiment at ISOLDE a study the decay of ${}^{16}\text{N}$ with the aim of obtaining a high-precision determination of the branching ratio on an absolute scale, will be done.

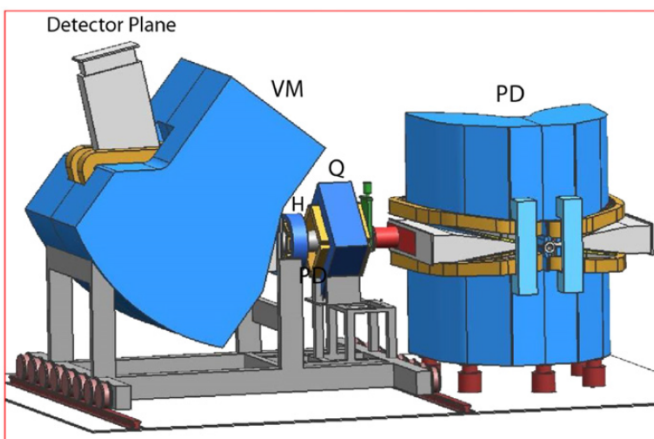


Fig. 27. Overview of the complete ELISe spectrometer system consisting of the pre deflector and the following QHD magnet system with a vertical-bending dipole. From Ref. [66].

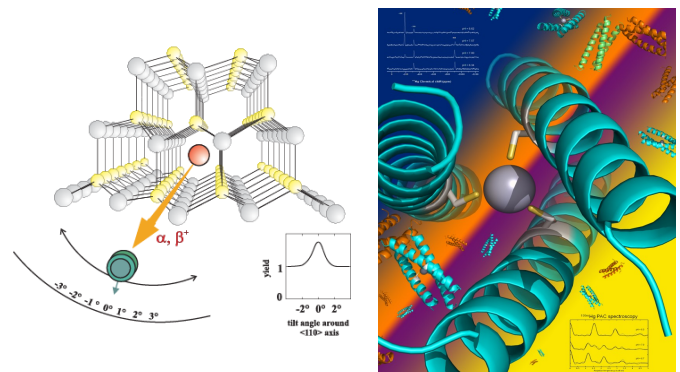


Fig. 28. Nuclear solid-state physics and biophysics.

3.3.2 Applications

A very vital program in nuclear solid-state physics has been conducted at CERN ISOLDE since the end of the seventies. This programme aims at studies of semiconductors, surfaces, magnetic materials and biomaterial. The techniques used are, for example, perturbed angular correlations (PAC), Mössbauer spectroscopy, nuclear orientation, diffusion, blocking and channeling (the latter illustrated to the left in Fig. 28 (see also Ref. [69]). The cartoon to the right symbolises studies of bio-molecules using PAC techniques with implanted ^{199m}Hg as probes [70].

Another applied project is CERN-MEDICIS, a project that will produce radioactive isotopes by recovering the proton beam before it reaches the beam dump, using different types of targets behind the ISOLDE targets. CERN-MEDICIS will form a symbiotic relationship with ISOLDE, taking advantage of the latter's unique ability, and experience to provide exotic carrier-free isotopes. Since advanced medical applications rely on the use of specific isotopes the target material is crucial for achieving significant production. During its initial stage in 2016 the production will be limited to $^{44,47}\text{Sc}$ and $^{61,64}\text{Cu}$. In the second stage, tentatively in 2017, targets from the nuclei of higher atomic numbers, such as tantalum foils, reaching some of the most interesting terbium and lanthanide isotope and in a final phase in 2018, the use of uranium carbide would give an even wider range of isotopes.

4 Final remark

Let me end my contribution to our school in the same way as I started my speech at the 2012 Nobel Ceremony, with some words quoted from the epilogue at the Master's Degree Celebration in Lund, Sweden in 1820, by Professor Esaias Tegnér – also a famous poet and author – who said

*This is Man's wonderful ability
to be able to grasp the inner essence of phenomena,
not what they appear to be, but what they mean,
and the reality that we see with our eyes
a symbol only of something higher.*

Finally I would like to thank all that contributed to the success of this school, and in particular Angela, who took the initiative. Let Fig. 29 be a symbol and inspiration for the continuation of re-writing of Nuclear Physics Textbooks.

References

1. I. Tanihata *et al.*, Phys. Rev. Lett. **55** (1985) 2676.
2. P.G. Hansen, B. Jonson, Europhys. Lett. **4** (1987) 409.
3. R. Kanungo *et al.*, Phys. Rev. Lett. **114** (2015) 192502.
4. www.nscl.msu.edu/thoennes/isotopes/
5. O. Kofoed-Hansen, K.O. Nielsen, Phys. Rev. **82** (1951) 96.
6. O. Kofoed-Hansen, Thesis University of Copenhagen, in Danish.
7. B. Pontecorvo, Sov. Phys. JEPT **26** (1968) 493.
8. V.N. Gribov, B. Pontecorvo, Phys. Lett. B **28** (1969) 493.
9. Y. Fukuda *et al.* Phys. Rev. Lett. **81** (1998) 1562.
10. Q.R. Ahmad *et al.*, Phys. Rev. Lett. **87** (2001) 071301.
11. Q.R. Ahmad *et al.*, Phys. Rev. Lett. **89** (2002) 011301.
12. www.nobelprize.org/nobel_prizes/physics/laureates/2015/advanced-physicsprize.pdf
13. K. Blaum, M.J.G. Borge, B. Jonson, P. Van Duppen, in *60 years of CERN Experiments and Discoveries* Eds. H. Schopper, L. Di Lella, *Advanced series on Directions in High Energy Physics* Vol. **23** (World Scientific) p. 415.
14. Proceedings of the Lysiekil Conference, Arkiv för Fysik, **36** (1967) 1- 686.
15. J. Blomqvist, Arkiv för Fysik, **36** (1967) 681.
16. P.G. Hansen *et al.*, Phys. Lett. B **28** (1969) 415.
17. J. Bonn *et al.*, Phys. Lett. B **38** (1972) 308.
18. M.D. Seliverstov *et al.*, Phys. Lett. B **719** (2013) 362.
19. T.J.M. Symons *et al.*, Phys. Rev. Lett. **42** (1979) 40.
20. G.D. Westfall *et al.*, Phys. Rev. Lett. **43** (1979) 1859.
21. T.J.M. Symons, in: Proc. Int. Conf. on Nucl. far from Stability, Helsingør (1981), CERN 81-09 (1981) 668.
22. A.M. Poskanzer *et al.*, Phys. Rev. Lett. **17** (1966) 1271.
23. K.H. Wilcox *et al.*, Phys. Lett. B **59** (1975) 142.
24. C. Thibault *et al.*, Phys. Rev. C **12** (1975) 644.
25. E. Roeckl *et al.*, Phys. Rev. C **10** (1974) 1181.
26. R.E. Azuma *et al.*, Phys. Rev. Lett. **43** (1980) 31.
27. R.E. Azuma *et al.*, Phys. Lett. B **96** (1979) 1652.
28. Maria J.G. Borge, Marcelle Epherre-Rey-Campagnolle, Dominique Guillemaud-Mueller, B. Jonson, M. Langevin, G. Nyman and Catherine Thibault, Nucl. Phys. A **460** (1986) 373.
29. P.G. Hansen, B. Jonson, in: *Particle Emission from Nuclei*, Vol. III, CRC Press, Inc. (1989) p. 157, Eds. D.N. Poenaru and M.S. Ivascu.
30. M. Pfützner, Phys. Scr. **T152** (2013) 014014.
31. O. Kester *et al.*, Nucl. Instr. & Meth. B **204** (2003) 20.
32. Y. Blumenfeld, N. Nilsson, P. Van Duppen, Phys. Scr. **T152** (2013) 014023.
33. A. Gade, C.K. Gelbke, Scholarpedia (2010) 5(1):9651.
34. M. Pfützner *et al.*, Phys. Rev. C **92** (2015) 014316.
35. K. Blaum, J. Dilling, W. Nörtherhäuser, Phys. Scr. **T152** (2013) 014017.
36. M. Smith *et al.*, Phys. Rev. Lett. **101** (2008) 202501.
37. A.T. Gallant *et al.*, Phys. Rev. Lett. **113** (2014) 082501.
38. B.E. Glassman *et al.*, Phys. Rev. C **92** (2015) 042501.
39. W. Nörtherhäuser *et al.*, Phys. Rev. Lett. **102** (2009) 062503.

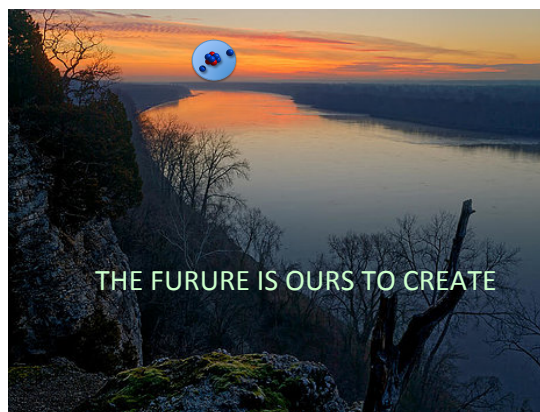


Fig. 29. Courtesy Robert Charity.

40. A. Krieger *et al.*, Phys Rev. Lett. **108** (2012) 142501.
41. J.C. Hardy, P.G. Hansen, B. Jonson, Phys. Lett. B **71** (1977) 307.
42. J.C. Hardy, B. Jonson, P.G. Hansen, Nucl. Phys. A **305** (1978) 15.
43. E.P. Wigner, *Results and theory of resonance absorption* in Oak Ridge Natl. Lab. Rept. ORNL-2309.
44. C.E. Porter and R.G. Thomas, Phys. Rev. **104** (1956) 483.
45. P.G. Hansen, B. Jonson, A. Richter, Nucl. Phys. A **518** (1990) 13.
46. T.E.O Ericson, Ann. Of Phys. **23** (1963) 390.
47. B. Jonson, *et al.*, Proc . 3rd Int. Conf. on nuclei far from stability, Cargse, 1976 (CERN 76-13, 1976) p .277.
48. T. Aumann *et al.*, Phys. Rev. C **59** (1999) 1252.
49. Sonia Bracca *et al.*, Phys Rev. Lett. **89** (2002) 052502.
50. K. Riisager, Phys. Scr. **T152** (2013) 014001.
51. M. Takechi *et al.*, Phys. Lett. B **707** (2012) 357
52. K. Riisager *et al.*, Phys. Lett. B **732** (2014) 305.
53. M.V. Zhukov *et al.*, Phys. Lett. B **244** (1990) 357.
54. B. Jonosn, Phys. Rep. **239** (2004) 1.
55. H. Simon, Phys. Scr. **T152** (2013) 014024.
56. Yu. Aksyutina *et al.*, Phys. Rev. C **87** (2013) 064316.
57. A. Bonaccorso, Phys. Scr. **T152** (2013) 014019.
58. R. Charity *private communication* 2015.
59. K. W. Brown *et al.*, Phys. Rev. Lett. **113** (2014) 232501.
60. J. Marganec *et al.*, Eur. Phys. J. A **51** (2015) 9.
61. K. W. Brown *et al.*, Phys. Rev. C **92** (2015) 034329.
62. I. Mukha *et al.*, Phys. Rev. Lett. **99** (2007) 182501.
63. I. Mukha *et al.*, Phys. Rev. C. **77** (2008) 061303.
64. M. Wakasugi *et al.*, Nucl. Instrum. Meth. B **317** (2013) 668.
65. A.N. Antonov *et al.*, Nucl. Instrum. Meth. A **637** (2011) 60.
66. T. Adachi *et al.*, Nucl. Instrum. Meth. A **659** (2011) 198.
67. H.O.U. Fynbo, Phys. Scr. **T152** (2013) 014010.
68. K. Langanke, H. Schats, Phys. Scr. **T152** (2013) 014011.
69. U. Whal, Nucl. Instrum. Meth. B **269** (2011) 3014.
70. O. Iranzo, Chem. Eur. J. **33** (2007) 9178.